frontiers | Frontiers in Chemistry

TYPE Original Research
PUBLISHED 18 October 2022
DOI 10.3389/fchem.2022.1005684

OPEN ACCESS

EDITED BY
Piotr Pander,
Silesian University of Technology, Poland

REVIEWED BY
Filippo Tamassia,
University of Bologna, Italy
Sergey V. Krasnoshchekov,
Lomonosov Moscow State University, Russia

*CORRESPONDENCE
O. O Panchenko,
panchenko9b@gmail.com

SPECIALTY SECTION
This article was submitted to Inorganic Chemistry, a section of the journal Frontiers in Chemistry

RECEIVED 28 July 2022
ACCEPTED 22 September 2022
PUBLISHED 18 October 2022

CITATION
Minaev BF, Panchenko OO, Minaeva VA and Ågren H (2022), Triplet state harvesting and search for forbidden transition intensity in the nitrogen molecule. *Front. Chem.* 10:1005684. doi: 10.3389/fchem.2022.1005684

Triplet state harvesting and search for forbidden transition intensity in the nitrogen molecule

B. F Minaev[1,2], O. O Panchenko[1]*, V. A Minaeva[1] and H Ågren[2]

[1]Department of chemistry and nanomaterial sciences, Bohdan Khmelnytsky National University, Cherkasy, Ukraine, [2]Department of Physics and Astronomy, Uppsala University, Uppsala, Sweden

Triplet excited states of the N_2 molecule play an important role in electric discharges through air or liquid nitrogen accompanied by various afterglows. In the rarefied upper atmosphere, they produce aurora borealis and participate in other energy-transfer processes connected with atmospheric photochemistry and nightglow. In this work, we present spin–orbit coupling calculations of the intensity of various forbidden transitions, including the prediction of the electric dipole transition moment of the new $1^3\Sigma_g^- \leftarrow A^3\Sigma_u^+$ band, which is strongly prohibited by the (+|–) selection rule, the new spin-induced magnetic $B'^3\Sigma_u^- \leftarrow A^3\Sigma_u^+$ transition, magnetic and electric quadrupole transitions for the $B^3\Pi_g \leftarrow X^1\Sigma_g^+$ Wilkinson band, and the Lyman–Birge–Hopfield $a^1\Pi_g \leftarrow X^1\Sigma_g$ transition. Also, two other far-UV singlet–singlet quadrupole transitions are calculated for the first time, namely, the Dressler–Lutz $a''^1\Sigma_g^+ - X^1\Sigma_g^+$ and the less studied $z^1\Delta_g - X^1\Sigma_g^+$ weak transitions.

KEYWORDS

triplet–singlet transitions, nitrogen molecule, Vegard–Kaplan band, Wilkinson band, Herzberg I band analog

Introduction

The great flux of solar energy through the upper atmosphere can be harvested by the rarefied gases of molecular and atomic components of the Earth's mesosphere and lower thermosphere (MLT) regions (Minaev and Panchenko, 2020). The ground states of such abundant O_2 ($^3\Sigma_g^-$), O (^{3}P), and N (^{4}S) species of MLT possess high multiplicity, and thus their lowest excited states are metastable, having a low electronic spin and strongly forbidden radiative relaxation (Wilkinson and Mulliken, 1959; Brown and Winkle, 1970; Minaev and Panchenko, 2020). Their long-lived emission to the ground state provides the possibility to harvest visible and near-UV solar radiation engaged in various energy transfer processes, which determine the climate, meteorology, and weather conditions (Minaev and Panchenko, 2020). In contrast, the ground state of the nitrogen molecule possesses zero spin and several high-energy triplet excited states with deep potential wells. The lowest of them, $A^3\Sigma_u^+$, can harvest a stock of 6.22 eV energy, being a strongly metastable triplet state with a relatively long radiative lifetime (τ_r) of 2 s (Brown and

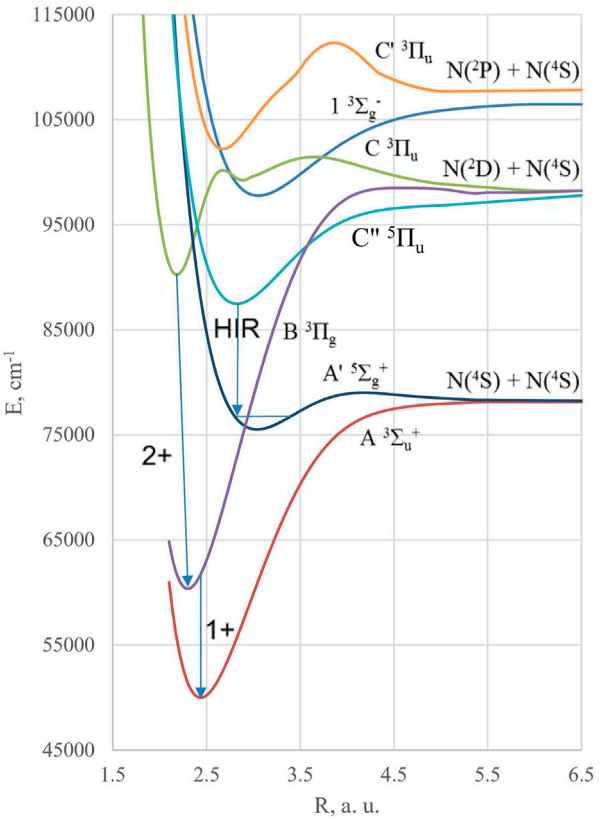

FIGURE 1
Potential energy curves of several spectroscopy important excited states of the N_2 molecule. The first (**1+**) and second positive (**2+**) systems are denoted together with the Herman infrared (HIR) emission band.

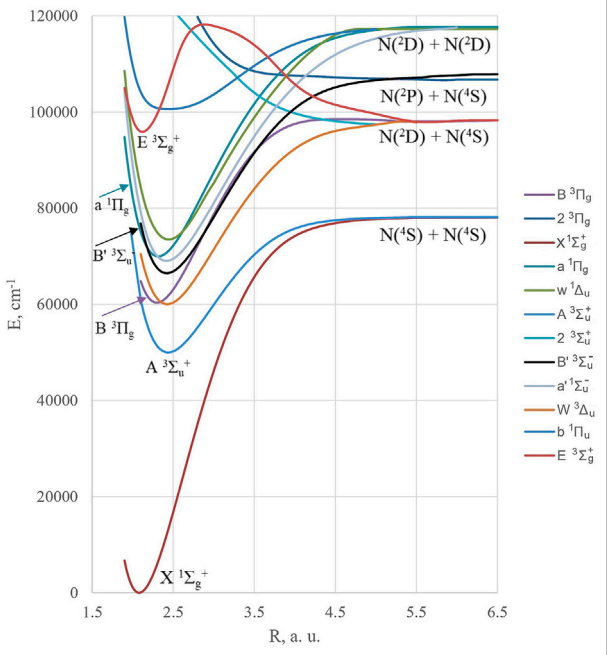

FIGURE 2
Low-lying bound states, which contribute to the intensity of the studied transition.

Winkle, 1970; Minaev et al., 1995; Begley et al., 2022). Accounting for the short UV wavelength of the $A^3\Sigma_u^+ \rightarrow X^1\Sigma_g^+$ transition, this τ_r value is indeed unusually large.

N_2 is a very stable and inert molecule in the ground state $X^1\Sigma_g^+$ with high dissociation energy (D_e = 9.76 eV). At the same time, N_2 possesses a variety of quite stable valence excitations of the π_u–π_g and $3\sigma_g$–π_g types; these excited states have large D_e values (around 4–6 eV) and are mostly metastable since their emission to the ground state is strictly forbidden by the electric dipole selection rules (Wilkinson and Mulliken, 1959; Brown and Winkle, 1970; Begley et al., 2022; Minaev et al., 1995; Lewis et al., 2008; Lofthus. and Krupenie, 1977). In gaseous electric discharges, when a molecule is irradiated by an electron flux, N_2 dissociates into the ground state N (^{4}S) atoms; they can recombine forming the lowest singlet ($X^1\Sigma_g^+$), triplet ($A^3\Sigma_u^+$), and quintet ($A'^5\Sigma_g^-$) basic states. The last two, shown in Figure 1, are involved in the so-called active nitrogen phenomenon detected by the characteristic "yellow afterglow" (Brown and Winkle, 1970; Begley et al., 2022). Its study together with aurora borealis involves a large number of metastable states and forbidden transitions in the N_2 spectrum (Figure 2). The Lewis–Rayleigh afterglow (Brown and Winkle, 1970) in the discharge consists of the first positive system of the nitrogen molecule, extending from IR to the blue edge, being the triplet–triplet $B^3\Pi_g \rightarrow A^3\Sigma_u^+$ transition (**1+** system) (Lofthus. and Krupenie, 1977). The visible part of the **1+** system was already investigated in 1902 by Deslandres (1902); *ab initio* interpretation of its intensity was achieved by Werner et al. (1984) and a final form by Ni et al. (2017). It should be distinguished from the second positive system of the nitrogen molecule—the $C^3\Pi_u \rightarrow A^3\Sigma_u^+$ transition (**2+** system) and the infrared Hermann (HIR) band $C''^5\Pi_u \rightarrow A'^5\Sigma_g^+$ (Figure 1). The main sources of emission of the first and second positive systems in N_2 discharge are connected with the involvement of the N (^{2}D) excited atom into a recombination reaction (Figure 1). The **2+** band system was observed as early as 1869 as it readily appears in ordinary air discharges (Deslandres, 1902), but its rovibronic assignment came much later (Lofthus and Krupenie, 1977). As opposed to the O_2 molecule (Minaev and Panchenko, 2020), many visible and UV transitions between triplet excited states generated by electric discharge are possible in the nitrogen counterpart (Lofthus. and Krupenie, 1977; Minaev et al., 1995; Lewis et al., 2008). The quintet state $A'^5\Sigma_g^+$ and the HIR system of N_2 have become clear only recently (Partridge et al., 1988; Hochlaf et al., 2010a). They are essentially important for the recombination of the N (^{4}S) ground state atoms being the precursor of the Lewis–Rayleigh afterglow. The quintet $A'^5\Sigma_g^+$

can predissociate to the $B^3\Pi_g$ state vibrational levels (v = 10–12, Figure 1), though the spin–orbit coupling (SOC) matrix element (ME) $<A'^5\Sigma_g^+|H_{so}|\ B^3\Pi_g>$ is rather weak near the crossing in order to be efficient for generation of the spontaneous **1+** emission in the recombination of N (^{4}S) atoms. At the same time, this SOC ME determines the high radiative probability (Einstein coefficient about $3{\cdot}10^4$ s^{-1}) of the newly predicted $A'^5\Sigma_g^+ \rightarrow A^3\Sigma_u^+$ (0–6) transition, which borrows intensity from the **1+** system, as well as from the HIR band (Minaev et al., 2022). The latter source is attributed to a strong SOC between the $A^3\Sigma_u^+$ and $C''^5\Pi_u$ states.

The excited metastable N (^{2}D) and N (^{2}P) atoms with energies of 2.4 eV and 3.6 eV above the N (^{4}S) ground state, respectively (Figure 1), are present with low concentration in the discharge. Their recombination leads to a huge number of excited N_2 states with varying degrees of stability and spontaneous emission probabilities (Lofthus. and Krupenie, 1977). Several other important states of nitrogen are shown in Figure 2.

Energy harvesting by triplet states of nitrogen

The triplet excited manifold of the N_2 molecule is well studied in far-UV absorption and emission spectra (Deslandres, 1902; Lofthus. and Krupenie, 1977; Werner et al., 1984; Partridge et al., 1988; Piper, 1993; Minaev et al., 1995; Lewis et al., 2008; Ndome et al., 2008; Hochlaf et al., 2010a; Ni et al., 2017). In 1932, Vegard detected 120 weak bands in the red-degraded phosphorescence of solid nitrogen through the wide region of 670–170 nm (Lofthus and Krupenie, 1977). Soon after, Kaplan observed similar bands in an N_2 laboratory discharge (Minaev et al., 1995). The weak Vegard–Kaplan (VK) system was first detected by Wilkinson as absorption bands in a long-path spectrometer at 169 and 128 nm for highly excited vibronic levels (v' = 6,7) (Wilkinson and Mulliken, 1959). Later on, the VK rovibronic intensity alternations were measured and analyzed very carefully (Lofthus and Krupenie, 1977; Piper, 1993) including *ab initio* calculations for the VK transition probability and many other inter-combination systems (Minaev et al., 1995). SOC calculations within the quadratic response theory (Minaev et al., 1995) explained why the Ogawa–Tanaka–Wilkinson system $B'^3\Sigma_u^- \leftarrow X^1\Sigma_g^+$ is much more intense (70 times) than the Vegard–Kaplan $A^3\Sigma_u^+ \leftarrow X^1\Sigma_g^+$absorption and why the Tanaka transition $C^3\Pi_u \leftarrow X^1\Sigma_g^+$ is the most intense among all known triplet–singlet (T–S) absorption bands at that time (Lofthus and Krupenie, 1977; Minaev et al., 1995). The new T ← S transition $D^3\Sigma_u^+ \leftarrow X^1\Sigma_g^+$ in the far-UV region predicted by Minaev et al. (1995) was later detected and analyzed by Lewis et al. (2008). The upper $D^3\Sigma_u^+$ state has been observed earlier in the pure nitrogen condensed discharge afterglow through the $D^3\Sigma_u^+ \rightarrow B^3\Pi_g$ (0, v'') emission, which is now known as the fourth positive system (Lofthus and Krupenie, 1977; Minaev et al., 1995). The upper $D^3\Sigma_u^+$ state was shown to be of Rydberg type (Minaev et al., 1995) converging to the ground state N_2^+ ion. At longer N–N distances, it avoids crossing with the bound Rydberg state and the valence $3^3\Sigma_u^+$ state potential energy curve (PEC), demonstrating a repulsive character (Minaev et al., 1995). All theoretical predictions of the inter-combination D ← X transition (Minaev et al., 1995) have mainly been supported by later experiments (Lewis et al., 2008). The predicted 0–0 transition is rather intense (f = $2{\times}10^{-5}$), being the strongest inter-combination of a nitrogen molecule in agreement with measurements (Lofthus and Krupenie, 1977; Lewis et al., 2008). This far-UV region in N_2 absorption is very dense, being covered by allowed transitions ($b^1\Pi_u$–X, for example) (Lofthus and Krupenie, 1977), but the D–X (0, 0) band has a clear location in a fortuitous region of the $b^1\Pi_u \leftarrow$ X allowed spectrum, just above its (4,0) band head, enabling the D–X (0, 0) observation (Lewis et al., 2008). All three sublevels of the triplet D state provide four rotational branches in agreement with Minaev et al. (1995), according to rotational and parity selection rules of Hund's case "b" (Lewis et al., 2008). The small negative zero-field splitting (λ = −0.036 cm^{-1} (Lewis et al., 2008)) of the $D^3\Sigma_u^+$ state is in agreement with SOC and spin–spin coupling calculations (λ = −0.041 cm^{-1}) within the response approach (Loboda et al., 2003; Hochlaf et al., 2010b; Qin et al., 2019; Minaev et al., 2022).

Thus, almost all important singlet–triplet transitions in the molecular nitrogen absorption spectra (up to the far-UV region) from the ground state $X^1\Sigma_g^+$ to the triplet states of the "ungerade" symmetry—the $A^3\Sigma_u^+$, $B'^3\Sigma_u^-$, $W^3\Delta_u$, $C^3\Pi_u$, and $D^3\Sigma_u^+$ states—have been calculated by the quadratic response theory within the multi-configuration approach (Minaev et al., 1995), giving results that are in good agreement with experimental intensity distributions (Lofthus. and Krupenie, 1977; Piper, 1993; Lewis et al., 2008). The present work aims to calculate new forbidden transitions in the nitrogen spectra which have not been observed so far but can influence the triplet state harvesting and total kinetic balance of the upper atmosphere.

The $B^3\Pi_g$ state produced by the second and fourth positive systems (Lofthus and Krupenie, 1977) can further generate **1+** bands, and the lowest triplet $A^3\Sigma_u^+$ state by the cascade in the positive column of electric discharge. We have to note that the $B^3\Pi_g \rightarrow X^1\Sigma_g^+$ phosphorescence was not calculated in Minaev et al. (1995), since even an account of SOC cannot overcome its parity prohibition in terms of electric dipole selection rules. The calculation of this transition intensity is an aim of the present work.

The VK transition satisfies the orbital electric dipole selection rule (EDSR) (Minaev et al., 1995), but being spin-forbidden it cannot be effectively induced by direct UV absorption. Thus, the N_2 (A) state is primarily populated by collisions—in laboratory discharge and the upper atmosphere, this is accomplished through the electron impact and the cascade in the first

positive system. The relatively long radiative lifetime enables N_2 ($A^3\Sigma_u^+$) to participate in collisions with the main background gases of the MLT region and to produce chemical reactions with N_2, O_2, N, and O species. In particular, the reactions

$$N_2\left(A^3\Sigma_u^+\right)+O\left(^3P\right) = NO\left(X^2\Pi\right) + N^2\,(D)$$
$$N_2\left(A^3\Sigma_u^+\right)+O\left(^3P\right) = N_2\left(X^1\Sigma_g^+\right)+O\left(^1S\right)$$

are the most important ones (Yonker and Bailey, 2019). A recent steady-state MLT model developed for the N_2 ($A^3\Sigma_u^+$) vibrational distribution in the terrestrial atmosphere is supported by comparison with the Vegard–Kaplan dayglow emission from atmospheric photochemistry and ionospheric spectroscopy measurements (Yonker and Bailey, 2019). The steady-state N_2 ($A^3\Sigma_u^+$, *v*) vibrational distribution in the MLT region is found to be shifted to higher (v > 6) levels. This is in agreement with the VK absorption (Minaev et al., 1995) and is important for our study. Direct excitation from the ground N_2(X) state by the electron impact provides an essential contribution to populating the N_2 (A, v > 6) sublevels, though their dominant excitation mechanism is the radiative cascade *via* the **1+** system (Bruna and Grein, 2009; Yonker and Bailey, 2019; Ajello et al., 2020). The efficiency of this cascade depends on the $B^3\Pi_g \rightarrow X^1\Sigma_g^+$ transition intensity, which in turn is determined by the EDSR-forbidden $a^1\Pi_g \rightarrow X^1\Sigma_g^+$ magnetic-dipole-allowed band system. Intensity calculations of these strongly forbidden transitions are also the purpose of our work.

The N_2 molecule, the most common and abundant component of the air, plays a crucial role in many high-energy photochemical processes caused by solar radiation in the upper atmosphere (Yonker and Bailey, 2019; Ajello et al., 2020). The discovery of new N_2 transitions forbidden by the spin-selection rule and induced by SOC perturbation is an important part of optical nitrogen monitoring at different altitudes. The intensity origin of the known emission bands that are forbidden by the electric dipole selection rules is also an important task of N_2 spectroscopy (Deslandres, 1902; Wilkinson and Mulliken, 1959; Brown and Winkle, 1970; Lofthus and Krupenie, 1977; Werner et al., 1984; Partridge et al., 1988; Piper, 1993; Minaev et al., 1995; Lewis et al., 2008; Ndome et al., 2008; Hochlaf et al., 2010a; Ni et al., 2017; Begley et al., 2022). This work presents multi-reference configuration interaction (MRCI) calculations of the highly excited states of the nitrogen molecule and an explanation of the intensity origin of several forbidden optical transitions. With this aim and background, we have predicted the electric dipole transition moment (EDTM) of the unknown forbidden transition $1^3\Sigma_g^- - A^3\Sigma_u^+$ and calculated its dependence on the internuclear distance. This is a triplet–triplet (T–T) band, the intensity of which is entirely determined by spin–orbit coupling perturbations between various spin sublevels of the T states as was preliminarily shown in a recent work (Minaev et al., 2022). The upper $1^3\Sigma_g^-$ state was earlier calculated by similar MRCI methods (Hochlaf et al., 2010b; Qin et al., 2019), but no experimental manifestations of its existence have been evidenced so far, although the $1^3\Sigma_g^-$ state is predicted with a deep minimum (D_e = 1.23 eV) and high energy above the ground state (T_e = 12.15 eV) (Qin et al., 2019). We believe that the $1^3\Sigma_g^-$ state can be produced by N (^{2}P) + N (^{4}S) recombination (Figure 1), and that its low vibrational levels can avoid pre-dissociation at low pressure. The $N_2(1^3\Sigma_g^-)$ state possesses a potential energy well located outside the Franck–Condon (FC) region, which is accessible from the metastable $A^3\Sigma_u^+$ state as well as from the ground state. This explains the difficulties with the observation of the corresponding absorption bands. Under these conditions, the emissive $1^3\Sigma_g^- \rightarrow A^3\Sigma_u^+$ transition from the lowest v' = 0 sublevel will have the maximum FC factor for the v" = 7–8 vibronic levels of the *A* state. We provide evidence for the existence of this new band in the N_2 molecule by calculating the transition probabilities through an account of SOC in the first order of the perturbation theory and comparing them with other known forbidden transitions to facilitate the validity of such a prediction. This would be a wide band of low intensity in the range of 209–450 nm with an approximate maximum at 328 nm; it is prohibited by the severe selection rule (+) → (−) but is allowed by spin-selection as a T–T transition (Minaev et al., 2022). Its spin-rovibronic structure would be analogous to the well-known Herzberg I band of molecular oxygen $X^3\Sigma_g^- \rightarrow A^3\Sigma_u^+$ (Herzberg, 1952; Minaev and Muldakhmetov, 1984; Klotz and Peyerimhoff, 1986).

Intensity borrowing mechanisms of the forbidden $1^3\Sigma_g^- \rightarrow A^3\Sigma_u^+$ transition

For planning intensity calculations of the new band in nitrogen, we first take into account the corresponding well-known and intense transitions of the N_2 molecule, relevant for our purpose. According to SOC selection rules, the new N_2 band $1^3\Sigma_g^- \rightarrow A^3\Sigma_u^+$ can be formed by spin–orbit coupling-induced mixing of the upper state $1^3\Sigma_g^-$ with the $B^3\Pi_g$ state and by intensity borrowing from the first positive system $A^3\Sigma_u^+ - B^3\Pi_g$, see Eq. 1. To include the SOC effect, we have to add the Ω quantization, where $\Omega = L_z + S_z$ is the *z*-projection of the total electronic angular momentum and L_z and S_z are orbital and spin angular momenta projections on the molecular axis (Yonker and Bailey, 2019). The SOC operator can mix states with the same Ω; the EDTM selection allows transitions according to the rule $\Delta\Omega = 0, \pm1$:

$$\left|1^3\tilde{\Sigma}_{g,1}^-\right\rangle = \left|1^3\Sigma_{g,1}^-\right\rangle + \frac{\left\langle B^3\Pi_{g,1}\left|H_{SO}\right|1^3\Sigma_{g,1}^-\right\rangle}{E\left(1^3\Sigma_g^-\right) - E\left(B^3\Pi_g\right)}\left|B^3\Pi_{g,1}\right\rangle$$
$$= \left|1^3\Sigma_{g,1}^-\right\rangle + C_{B,1}\left|B^3\Pi_{g,1}\right\rangle,$$

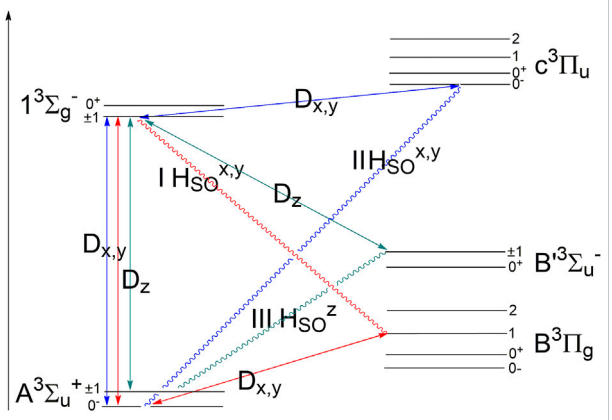

FIGURE 3
Scheme of intensity borrowing for the forbidden $\Sigma_g^- \rightarrow \Sigma_u^+$ transition. The first and second mechanisms provide perpendicular polarization, and the third one is responsible for the parallel polarization along the N–N axis.

$$\langle A^3\Sigma_{u,0^-}^+ | er | 1^3\tilde{\Sigma}_{g,1}^- \rangle = C_{B,1} \langle A^3\Sigma_{u,0^-}^+ | e\times | B^3\Pi_{g,1} \rangle, \quad (1)$$

Figure 3 presents this mechanism as the type "I SOC" mixing. By a similar SOC mechanism, the studied forbidden band can borrow EDTM intensity from the newly predicted $1^3\Sigma_g^- \rightarrow C^3\Pi_u$ transition here, Eq. 2; this SOC mechanism of intensity borrowing refers to the "II SOC" type in Figure 3. Both these mechanisms have the perpendicular *x, y* polarization of EDTM; only the *x* component is shown in Eqs. 1–2 for one sublevel of the degenerate Π states (Qin et al., 2019; Minaev et al., 2022).

$$|A^3\tilde{\Sigma}_{u,0^-}^+\rangle = |A^3\Sigma_{u,0^-}^+\rangle + \frac{\langle C^3\Pi_{u,0^-}|H_{SO}|A^3\Sigma_{u,0^-}^+\rangle}{E(A^3\Sigma_u^+) - E(C^3\Pi_u)}|C^3\Pi_{u,0^-}\rangle$$
$$= |A^3\Sigma_{u,0^-}^+\rangle + C_{C,A}|C^3\Pi_{u,0^-}\rangle,$$
$$\langle A^3\tilde{\Sigma}_{u,0^-}^+ | er | 1^3\Sigma_{g,1}^- \rangle = C_{C,A}^* \langle C^3\Pi_{u,0^-} | e\times | 1^3\Sigma_{g,1}^- \rangle. \quad (2)$$

Figure 3 provides a good explanation of the relevant intensity sources of the studied $1^3\Sigma_g^- \rightarrow A^3\Sigma_u^+$ transition, but it would be overloaded if all possible contributions are included. The type "II SOC" mechanism in Figure 3 includes also other states of the $C'^3\Pi_u$ type (in total five $^3\Pi_u$ states are taken into account).

An additional source of intensity borrowing denoted as the type "III SOC" mechanism in Figure 3 includes parallel EDTM for the studied emission band (light polarization along the molecular *z*-axis). By symmetry arguments, the $1^3\Sigma_g^- \rightarrow A^3\Sigma_u^+$ transition in N_2 is similar to the Herzberg I band of the O_2 molecule, and its probability can be calculated by a similar scheme of intensity borrowing (Minaev and Muldakhmetov, 1984; Klotz and Peyerimhoff, 1986). In the oxygen molecule, the main contribution to the absorption intensity of the Herzberg I band $X^3\Sigma_g^- \rightarrow A^3\Sigma_u^+$ origins from the SOC mixing between the $A^3\Sigma_{u,1}^+$ state and the upper term $B^3\Sigma_{u,1}^-$ of the Schumann–Runge system $X^3\Sigma_g^- \rightarrow B^3\Sigma_u^-$ (Minaev and Muldakhmetov, 1984), which is the most intense valence transition in molecular oxygen (Herzberg, 1952). This provides a rather unusual (for the $^3\Sigma^- – ^3\Sigma^+$ band) type of Ω = 1–Ω = 1 parallel transition intensity, though the ΔΩ = 1 selection rule is more typical for such bands with prevailing perpendicular polarization (Herzberg, 1952).

Let us consider the type "III SOC" mechanism in more detail. The SOC-induced mixing between the lowest $A^3\Sigma_u^+$ state and the upper triplet $B'^3\Sigma_u^-$ of the Ogawa–Tanaka–Wilkinson system ($B'^3\Sigma_u^- - X^1\Sigma_g^+$) can be presented by the perturbation theory in the form:

$$|A^3\tilde{\Sigma}_{u,1}^+\rangle = |A^3\Sigma_{u,1}^+\rangle + \frac{\langle B'^3\Sigma_{u,1}^-|H_{SO}|A^3\Sigma_{u,1}^+\rangle}{E(A^3\Sigma_u^+) - E(B'^3\Sigma_u^-)}|B'^3\Sigma_{u,1}^-\rangle$$
$$= |A^3\Sigma_{u,1}^+\rangle + C_{B',A}|B'^3\Sigma_{u,1}^-\rangle. \quad (3)$$

We can also account for SOC perturbation for the $1^3\Sigma_g^-$ counterpart as follows:

$$|1^3\tilde{\Sigma}_{g,1}^-\rangle = |1^3\Sigma_{g,1}^-\rangle + \frac{\langle E^3\Sigma_{g,1}^+|H_{SO}|1^3\Sigma_{g,1}^-\rangle}{E(1^3\Sigma_g^-) - E(E^3\Sigma_g^{-+})}|E^3\Sigma_{g,1}^+\rangle$$
$$= |1^3\Sigma_{g,1}^-\rangle + C_{E,1}|E^3\Sigma_{g,1}^+\rangle. \quad (4)$$

The EDTM between the perturbed states (3) and (4) is equal to

$$\langle 1^3\tilde{\Sigma}_{g,1}^- | er | A^3\tilde{\Sigma}_{u,1}^+ \rangle = C_{E,1} * \langle E^3\Sigma_{g,1}^+ | ez | A^3\Sigma_{u,1}^+ \rangle$$
$$+ C_{B',A} \langle 1^3\Sigma_{g,1}^- | ez | B'^3\Sigma_{u,1}^+ \rangle. \quad (5)$$

This means that the (+|−) forbidden transition $1^3\Sigma_g^- - A^3\Sigma_u^+$ can borrow intensity from ED-allowed $E^3\Sigma_g^+ - A^3\Sigma_u^+$ and $1^3\Sigma_g^- - B'^3\Sigma_u^-$ transitions. The latter contribution is a formal symmetry analog of the Schumann–Runge O_2 transition. The SOC mixing mechanism shown in Eq. 3 is presented in Figure 3 by the intensity borrowing scheme "III-SOC". The SOC-induced mechanism from Eq. 4 is not shown in Figure 3 to avoid overloading. The SOC matrix element (ME) in Eq. 3 is equal to zero in a semi-empirical approximation with the neglect of differential overlap:

$$H_{SOC} = \sum_A \varsigma_A \sum_i \vec{l}_{A,i}\vec{s}_i = \sum_i \vec{B}_i\vec{s}_i, \quad (6)$$

where ς_A is the SOC constant for the valence shell of the A atom and $\vec{l}_{A,i}\vec{s}_i$ is a scalar product of the orbital and spin operators for the *i*th electron (Minaev and Muldakhmetov, 1984; Minaev et al., 1993). For the pure main configurations of the $A^3\Sigma_u^+$ and $B'^3\Sigma_u^-$ states, the SOC ME is equal to $\frac{1}{2}(B_{\pi_{u,x}\pi_{u,y}} - B_{\pi_{g,x}\pi_{g,y}})$; this expression is zero with the neglect of differential overlap since $B_{\pi_{u,x}\pi_{u,y}} = B_{\pi_{g,x}\pi_{g,y}}$ (Minaev and Muldakhmetov, 1984), but the account of overlap in normalization of the π_u and π_g molecular orbitals in the r-centroid approach (1.282 Å) leads to the different estimations $B_{\pi_{u,x}\pi_{u,y}}$ = 85 $cm^{-1}$and $B_{\pi_{g,x}\pi_{g,y}}$ = 60 cm^{-1}.

Thus, the SOC ME in Eq. 3 reaches a non-zero value of 12.5 cm^{-1}, which is rather close to the MRCI result. This scrutinized analysis shows the importance of the contribution expressed by Eq. 3 and the analogy with the Herzberg I Schumann–Runge transition coupling in the O_2 molecule (Minaev and Muldakhmetov, 1984). The denominator in Eq. 3 is rather small and homogeneously changes with r distance (Figure 3). Although the $1^3\Sigma_g^- - B'^3\Sigma_u^-$ transition is relatively weak in the N_2 molecule (EDTM = 0.026 ea_0 at r = 1.4 Å) (Qin et al., 2019), its contribution to the final EDTM of Eqs 1–5 is the largest. The EDTM of the $E^3\Sigma_g^+ - A^3\Sigma_u^+$ transition (the Herman–Kaplan band system (Lofthus. and Krupenie, 1977)) has a smaller value (0.017 and 0.0105 ea_0 at r = 1.28 and 1.4 Å, respectively) (Qin et al., 2019), as well as the SOC ME in Eq. 4 at these distances (5.2 cm^{-1}) (Hochlaf et al., 2010b).

We have stressed before the EDTM component of the studied intensity borrowing from the $1^3\Sigma_g^- \rightarrow B'^3\Sigma_u^-$ band, which is a formal analog of the Schumann–Runge system of oxygen (Minaev and Panchenko, 2020). Thus, we can compare various contributions to the intensity of this so-far unknown transition with the well-known data for O_2 and N_2 spectra (Herzberg, 1952; Lofthus. and Krupenie, 1977; Minaev et al., 1995; Lewis et al., 2008). The intensity borrowing contribution from the first positive system $B^3\Pi_g \rightarrow A^3\Sigma_u^+$ in Eq. 1 can be compared with the Vegard–Kaplan S–T transition intensity presented in Eq. 7 (Minaev et al., 1995), which explains an extremely low spontaneous emission of the VK system.

$$< X^1\tilde{\Sigma}_g^+|er|A^3\tilde{\Sigma}_u^+ \geq = C_{X,B} < B^3\Pi_g|er|A^3\Sigma_u^+ > + C_{b,A} < b^1\Pi_u|er|X^1\Sigma_g^+ >, \quad (7)$$

$$C_{X,B} = \frac{< X^1\Sigma_g^+|H_{so}|B^3\Pi_g >}{E\left(B^3\Pi_g\right) - E\left(X^1\tilde{\Sigma}_g^+\right)}, \quad C_{b,A} = \frac{< b^1\Pi_u|H_{so}|A^3\Sigma_u^+ >}{E\left(A^3\Sigma_u^+\right) - E\left(b^1\Pi_u\right)}.$$

As shown in Figure 2, the two denominators in Eq. 7 have opposite signs. The first denominator E(B)–E(X) decreases with r distance prolongation, whereas the second one, E(A)–E(b), increases by an absolute value with r. In the vicinity of the ground state equilibrium r_e distance (1.098 Å), both contributions tend to cancel each other, and the EDTM value crosses the zero point (Minaev et al., 1995). In the whole FC region, the EDTM is still close to zero, and the VK system has very low intensity both in absorption and emission. Although both the SOC ME values in the nominators of Eq. 7 are rather large (Bruna and Grein, 2009; Hochlaf et al., 2010b) as well as the transition moments of the **1+** and $b^1\Pi_u \rightarrow X^1\Sigma_g^+$ systems (Qin et al., 2019), the cancellation of the two big terms in Eq. 7 is the only reason for the relatively large lifetime of the $N_2(A^3\Sigma_u^+)$ state. To a large extent, this is also the reason for the efficient solar energy harvesting by the triplet states of nitrogen molecules and the aurora borealis phenomena.

For the studied transition $1^3\Sigma_g^- \rightarrow A^3\Sigma_u^+$, only the first "I SOC" mechanism provides an essential sign change with the internuclear distance (Figure 4). In the FC region, no big cancellations of different sign contributions are shown. The deteriorating "I SOC" mechanism is rather weak in the FC region 1.28–1.62 Å. For the most intense 0–7 vibronic band, the calculated EDTM is equal to 1.41×10^{-4} ea_0, which corresponds to the radiative rate constant of 2.48 s^{-1}. The total radiative lifetime of the zero vibrational sublevel of the $1^3\Sigma_g^-$ state is estimated as 0.34 s.

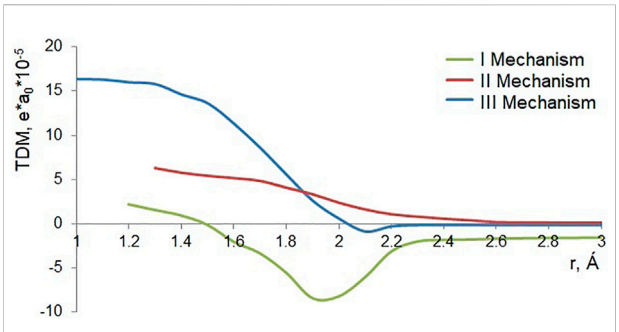

FIGURE 4
Transition dipole moment contributions of the $1^3\Sigma_g^- \rightarrow A^3\Sigma_u^+$ band system of the N_2 molecule according to three mechanisms shown schematically in Figure 3.

The $1^3\Sigma_g^-$ state can degrade much faster in the allowed T–T transitions (for example, through the $1^3\Sigma_g^- \rightarrow B'^3\Sigma_u^-$ emission). Thus, our estimation of the emissive $1^3\Sigma_g^- \rightarrow A^3\Sigma_u^+$ transition is definitely negative. However, in absorption, the same $A^3\Sigma_u^+(v''=7) \rightarrow 1^3\Sigma_g^-(v'=0)$ transition can be observable since the calculated oscillator strength (f_{7-0} = 2.23*10^{-9}) can be measured by modern techniques.

It is, at this point, relevant to estimate the other EDSR-forbidden inter-combination $B^3\Pi_g \rightarrow X^1\Sigma_g^+$ transition of nitrogen (Wilkinson system) (Lofthus. and Krupenie, 1977), which so far has not been calculated by quantum chemical methods. This is a magnetic dipole transition that borrows intensity from the magnetic singlet–singlet counterpart $a^1\Pi_g \rightarrow X^1\Sigma_g^+$ (Lofthus. and Krupenie, 1977).

Calculations of magnetic and electric quadrupole transition intensity

The Lyman–Birge–Hopfield (LBH) band system ($a^1\Pi_g \rightarrow X^1\Sigma_g^+$) of the N_2 molecule has been carefully studied in measurements of cascade-induced UV radiation to determine the intensity of this emission (Lofthus. and Krupenie, 1977). The LBH band has readily been seen in absorption as well as in emission though it is EDSR-forbidden by parity selection. Its magnetic and quadrupole transition moments are provided in Figure 5. They are calculated here at the level of the time-dependent density functional theory (TD DFT) using the

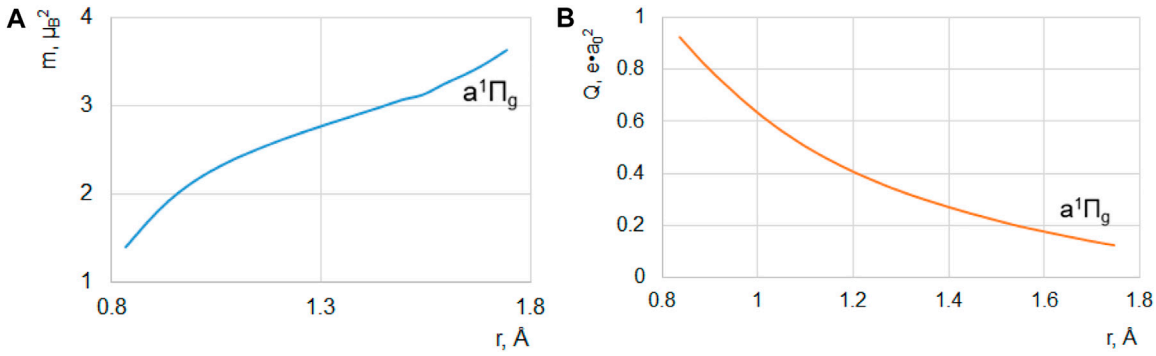

FIGURE 5
(A) Square of magnetic dipole moment $m_x^2+m_y^2$ (μ_B is the Bohr magneton) and **(B)** electric quadrupole moment of the $a^1\Pi_g$–$X^1\Sigma_g^+$ transition in the N_2 molecule (both in a. u.).

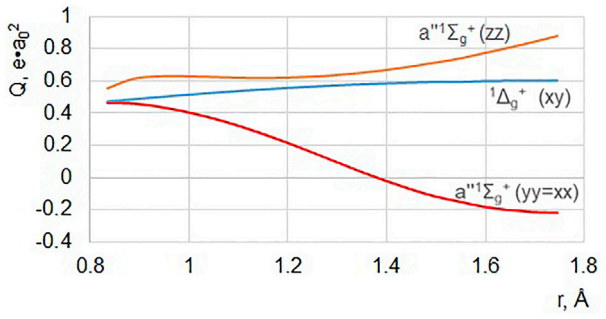

FIGURE 6
Electric quadrupole moment of the $a''^1\Sigma_g^+$–$X^1\Sigma_g^+$ transition in the N_2 molecule for all allowed components of the quadrupole tensor operator. The far-UV transition $^1\Delta_g$– $X^1\Sigma_g^+$ for the $Q_{XY} = Q_{YX}$ quadrupole tensor components are also presented (both in a. u.).

B3LYP functional and 6-311G++(*d, p*) basis set with the Gaussian-09 package (Frisch et al., 2010). We have studied 40 singlet states and triplet excited states of N_2 in the region 0.8–1.8 Å of the *r* distances. For the longer N–N bonds, the TD DFT approach produces untrustworthy PECs and cannot reproduce the proper dissociation limits. But for short *r* distances, all potential energy curves are quite reasonable and qualitatively reproduce MRCI results (Dahl and Oddershede, 1986; Qin et al., 2019). This DFT method provides equilibrium bond lengths of 1.205 and 1.598 Å for the triplet ($B^3\Pi_g$) and quintet ($A'^5\Sigma_g^+$) states of nitrogen, respectively. The latter is more realistic (Hochlaf et al., 2010a), whereas the former r_e value deviates slightly from the experimental value of 1.213 Å (Lofthus. and Krupenie, 1977).

A similar approach has been successfully used for the permanent quadrupole moment calculations in N_2 (Dahl and Oddershede, 1986). In addition to the LBH system, some other EDSR-forbidden bands are also calculated as quadrupole transitions, as shown in Figure 6. The Dressler–Lutz $a''^1\Sigma_g^+$–$X^1\Sigma_g^+$ quadrupole transition at 101 nm as well as the far-UV transition $z^1\Delta_g$–$X^1\Sigma_g^+$ (Figure 6) are calculated for the first time.

The growth of magnetic strength of the $a^1\Pi_g \rightarrow X^1\Sigma_g^+$ transition (Figure 5A) and the decrease of its quadrupole moment are notable (Figure 5B). The $a''^1\Sigma_g^+$– $X^1\Sigma_g^+$ transition moment represents a complicated tensor with *r*-dependent anisotropy (Figure 6).

In the FC region (1.1–1.3 Å), our results in Figure 5 well coincide with the calculations of Dahl and Oddershede, (1986) using the random phase approximation (RPA). The magnetic dipole transition moment (MDTM) of the LBH system (Figure 5A) increases with *r*, showing a trend of saturation at r = 1.3 Å, whereas the electric quadrupole transition moment (EQTM) decreases along the whole *r* range. Accounting for experimental FC factors and transition frequencies, we have obtained the radiative lifetime for the 0–0 vibronic transition of the LBH system equal to 65 μs in a reasonable agreement with experimental values in the interval 80–120 μs (Lofthus. and Krupenie, 1977; Dahl and Oddershede, 1986). The calculated magnetic to quadrupole intensity ratio (m/eq) is equal to 92%, whereas experimental data are in the range of 67%–96% interval (Dahl and Oddershede, 1986). Emission from the higher vibrational levels has a lower probability of qualitative agreement with observations (Lofthus. and Krupenie, 1977; Dahl and Oddershede, 1986). At the same time, we cannot accept the idea that the $a^1\Pi_g$ state can decay solely into the $X^1\Sigma_g^+$ ground state (Dahl and Oddershede, 1986). From Figure 2, one can see that the infrared $a^1\Pi_g \rightarrow a'^1\Sigma_u^-$ emission is possible; its electric dipole transition moment is equal to 0.2 ea_0 (Qin et al., 2019) using the *r*-centroid approach corresponding to the radiative lifetime for the 0–0 band of τ_r = 9 ms (FC factor is

0.219). We have also estimated a new quadrupole transition $a^1\Pi_g \rightarrow B^3\Pi_{g,1}$. Accounting for SOC, in Eq. 8, this transition moment origins in the difference in the permanent quadrupole moments of these two states: Q ($B^3\Pi_g$) = 0.59 ea_0^2 and Q ($a^1\Pi_g$) = 0.48 ea_0^2. This difference is small as well as the quadrupole moment of transition $a \rightarrow B$ ($4.9*10^{-4}$ ea_0^2), but in principle, we could not disregard branching emission into other lower lying triplet states (B', W, and A) in the calculation of the radiative lifetime of the LBH system. These S–T transitions are allowed in the EDSR approach with an account of spin–orbit coupling perturbation. Thus, we consider it more appropriate to present also the oscillator strength for the Lyman–Birge–Hopfield 0–0 band $a^1\Pi_g \leftarrow X^1\Sigma_g^+$ in absorption: $f_{0-0} = 7.24\times10^{-6}$.

The Dressler–Lutz $a''^1\Sigma_g^+$–$X^1\Sigma_g^+$ quadrupole transition in the far-UV absorption region (101 nm) is of the Rydberg type (Lofthus. and Krupenie, 1977); it is well reproduced by our TD DFT calculations. The triplet counterpart of the $a''^1\Sigma_g^+$ state is the known $E^3\Sigma_g^+$ Rydberg term, which was discussed previously when presenting our calculations of the Herman–Kaplan system ($E^3\Sigma_g^+ - A^3\Sigma_u^+$ transition). The Dressler–Lutz $a''^1\Sigma_g^+ \leftarrow X^1\Sigma_g^+$ band was observed in absorption at high pressure, and its intensity is mainly induced by collisions (Lofthus. and Krupenie, 1977). In this aspect, it is similar to the quadrupole Noxon band of O_2, which is very sensitive to collision-induced intensity enhancement (Minaev et al., 1994). Both $^1\Sigma_g^+$ states have similar r_e distance (about 1.1 Å) and FC factor close to unit. The calculated oscillator strength of the 0–0 band of the quadrupole $a''^1\Sigma_g^+ \leftarrow X^1\Sigma_g^+$ transition in nitrogen is equal to $1.5\cdot10^{-7}$, and it is detectable even at low pressure.

Now, we can estimate the probability of the latter triplet–singlet $B^3\Pi_g \leftarrow X^1\Sigma_g^+$ transition of the nitrogen molecule which, being strictly forbidden by ED selection, has not been included in previous calculations (Minaev et al., 1995). This Wilkinson band borrows intensity from the LBH band system ($a^1\Pi_g \leftarrow X^1\Sigma_g^+$) of the N_2 molecule because of the relatively strong spin–orbit coupling

$$< B^3\Pi_{g,1} | H_{so}^{x,y} | a^1\Pi_g > = 41.4\ cm^{-1}, \quad (8)$$

at the r_e distance and small energy gap between the B–a states. Only the $\Omega = 1$ spin sublevel of the triplet $B^3\Pi_{g,1}$ state is active in the Wilkinson band absorption, and its rotational structure supports the magnetic transition nature (Lofthus. and Krupenie, 1977). The SOC of Eq. 8 and m_1 magnetic moment (Figure 5A) provide the largest contribution (98.6%) to the $B^3\Pi_g \leftarrow X^1\Sigma_g^+$ transition intensity. The other $k^1\Pi_g$ state ($1\pi_u \rightarrow 3\sigma_u$) shows a smaller magnetic moment for the $k^1\Pi_g$–X transition ($m = 0.085\ \mu_B$) and a much smaller SOC counterpart at the B state equilibrium. Although both parameters increase with r, their relative contributions remain rather small. The calculated magnetic transition moment for the 0–0 band of the Wilkinson absorption $B^3\Pi_g \leftarrow X^1\Sigma_g^+$ is equal to 0.0073 μ_B. It corresponds to the oscillator strength $f_{0-0} = 2.54\cdot10^{-10}$, and the magnetic intensity remains dominant for this transition. It is not strange that Wilkinson (1962) used an optical path as long as 20 m to detect this band.

Finally, we have estimated the spin-induced magnetic dipole moment for a new $B'^3\Sigma_u^- - A^3\Sigma_u^+$ transition of the N_2 molecule. According to Eq. 3, the perturbed A state has a small B' state admixture for the $M_s = \pm1$ sublevels: $|A^3\Sigma_{u,1}^+\rangle + C_{B',A}|B'^3\Sigma_{u,1}^-\rangle$. Thus, the transition to the next $M_s = 0^+$ spin sublevel of the B' state $B'^3\Sigma_{u,0+}^- \leftarrow A^3\Sigma_{u,1}^+$ can borrow spin-current intensity from the microwave $B'^3\Sigma_{u,0}^- - B'^3\Sigma_{u,1}^-$ absorption band with the standard spin-magnetic transition moment that equals 2 μ_B. For the 0–0 absorption band $B'^3\Sigma_u^- \leftarrow A^3\Sigma_u^+$, we have obtained oscillator strength $f = 1.67 \cdot 10^{-12}$, which is probably possible for detection.

Conclusion

The presence of nitrogen atoms in the discharge afterglow classifies "active nitrogen" as a free-radical phenomenon. This is relevant to the aurora borealis' bright light and the yellow–orange Lewis–Rayleigh afterglow in the N_2 gas discharge. The spectrum consists of several triplet–triplet emission bands of the **1+** and **2 +** nitrogen systems ($B^3\Pi_g$–$A^3\Sigma_u^+$ and $C^3\Pi_u$–$B^3\Pi_g$ transitions) and the $B'^3\Sigma_u^- \rightarrow B^3\Pi_g$ infrared-visible afterglow system. The wide Wu–Benesh system $B^3\Pi_g = W^3\Delta_u$ is another T–T transition of the afterglow (Lofthus. and Krupenie, 1977). One can see that many triplet states of the nitrogen molecule take part in discharge afterglow together with numerous T–S transitions and S–S cascades. The transitions allowed by the electric dipole selection rule are nowadays accurately calculated by sophisticated *ab initio* methods (Qin et al., 2019) including many T–S vibronic bands induced by SOC perturbation (Minaev et al., 1995). This is important for the kinetic balance of triplet harvesting in discharges and the Earth's mesosphere and lower thermosphere regions. In the present work, we have calculated the probability of the magnetic and quadrupole Lyman–Berge–Hopfield transition $a^1\Pi_g \leftarrow X^1\Sigma_g^+$, which is necessary for the intensity estimation of the Wilkinson $B^3\Pi_g \leftarrow X^1\Sigma_g^+$ band (the only unknown intensity of a pure electronic T–S transition at zero pressure).

We have also calculated new transitions, $1^3\Sigma_g^- \leftarrow A^3\Sigma_u^+$ and $B'^3\Sigma_u^- \leftarrow A^3\Sigma_u^+$, that can be observed during absorption. The reason for finding such transitions is that the first excited triplet state $A^3\Sigma_u^+$ of N_2 possesses a relatively long radiative lifetime (about 2 s). Therefore, it is possible to excite the triplet–triplet transition from the $A^3\Sigma_u^+$ state by two-photon experiments or other methods of flash photolysis in discharge. We know that the Herzberg I transition was discovered in the oxygen molecule as an excitation from the ground state $X^3\Sigma_g^-$, but in nitrogen, the situation is reversed since the $1^3\Sigma_g^-$ symmetry corresponds to the upper state.

The $1^3\Sigma_g^-$ state, non-observed so far, has an electronic wave function, which is mainly represented by the valence configuration $(1\pi_u)^2$ $(1\pi_g)^2$ in a form similar to a quintet $A'^5\Sigma_g^+$ state. The quintet–triplet $A'^5\Sigma_g^+$–$A^3\Sigma_u^+$ transition, also induced by SOC in the electric dipole approach, is the most intense among all studied intercombinations. The spin-induced $B'^3\Sigma_u^- \leftarrow A^3\Sigma_u^+$ transition in the visible region is interesting since it is rather unique in magnetic-origin borrowing intensity from the electron spin resonance in the $B'^3\Sigma_u^-$ state. The transition intensity could be sensitive to the external magnetic field in solid nitrogen. The $B'^3\Sigma_u^- \leftarrow A^3\Sigma_u^+$ band in N_2 has common features

Transition	Absorption		Emission	Wavelength
$1^3\Sigma_g^- \rightarrow A^3\Sigma_u^+$	$f_{0,0} = 5.2\ 10^{-12}$	$f_{0,7} = 2.2\ 10^{-9}$	$\tau = 0.34$ s	$\lambda_{0,7} =$ 328 nm
$A'^5\Sigma_g^+$–$A^3\Sigma_u^+$	$f_{0,0} =$ $4.9\ 10^{-8}$	$f_{0,6} = 2.0\ 10^{-4}$	$\tau =$ 8.23 μs	$\lambda_{0,6} =$ 598 nm
$B'^3\Sigma_u^- \leftarrow A^3\Sigma_u^+$	$f_{0,0} = 1.6\ 10^{-12}$	Overlapped by 1 + band	$\tau = 3750$ s	$\lambda = 620$ nm

with the visible A-band of molecular oxygen (Minaev et al., 1994; Minaev and Minaeva, 2001).

Thus, we have noted many important comparable features in N_2 and O_2 spectra and also calculated for the first time the intensity of the predicted forbidden transitions including some magnetic dipole and quadruple S–S transitions in the nitrogen molecule. The main new predicted results are summarized in the following table.

Data availability statement

The raw data supporting the conclusion of this article will be made available by the authors, without undue reservation.

Author contributions

OP: writing small fragments of the text, computer calculations of molecules, development of drawings, and correction of the text. BM: main author of the manuscript, writing most of the text, development of drawings, and selection and processing of literary sources. VM: writing text fragments and text correction. HÅ: writing text fragments and processing computer calculations.

Funding

This work was supported by the Ministry of Science and Education of Ukraine (project 0122U000760) and by the Swedish Wenner-Gren Foundations (project GFU 2022–0036).

Acknowledgments

The authors express gratitude to Ramon S. da Silva and Majdi Hochlaf for useful discussions. Boris Minaev acknowledges a grant from the Wennergren-Foundations through their program for support of international reserach, grant no. GFU2022-0036. The authors thank the Swedish National Infrastructure for Computing (SNIC 2021-3-22 and SNIC 2022-5-103) at the National Supercomputer Centre of Linköping University and High-Performance Computing Center North (Sweden) partially funded by the Swedish Research Council through grant agreement no. 2018-05973.

Conflict of interest

The authors declare that the research was conducted in the absence of any commercial or financial relationships that could be construed as a potential conflict of interest.

Publisher's note

All claims expressed in this article are solely those of the authors and do not necessarily represent those of their affiliated organizations, or those of the publisher, the editors, and the reviewers. Any product that may be evaluated in this article, or claim that may be made by its manufacturer, is not guaranteed or endorsed by the publisher.

References

Ajello, J. M., Evans, J. S., Veibell, V., Malone, C. P., Holsclaw, G. M., Hoskins, A. C., et al. (2020). The UV spectrum of the Lyman-Birge-Hopfield band system of $N_2$is induced by cascading from electron impact. *J. Geophys. Res. Space Phys.* 125, e2019JA027546. doi:10.1029/2019JA027546

Begley, A. I., Shuman, N. S., Long, B. A., Kampf, R., Gyr, L., Viggiano, A. A., et al. (2022). Excited-state N atoms transform aromatic hydrocarbons into N-heterocycles in low-temperature plasmas. *J. Phys. Chem. A* 126 (10), 1743–1754. doi:10.1021/acs.jpca.1c10657

Brown, R., and Winkle, C. A. (1970). The chemical behavior of active nitrogen. *Angew. Chem. Int. Ed. Engl.* 9 (3), 181–196. doi:10.1002/anie.197001811

Bruna, P. J., and Grein, F. (2009). Theoretical study of electric moments, polarizabilities, and fine and hyperfine coupling constants of the $B^3\Pi_g$, $C^3\Pi_u$, $A'^5\Sigma_g^+$, and $C'^5\Pi_u$states of N_2//Can. *Can. J. Phys.* 87, 589–600. doi:10.1139/P09-011

Dahl, F., and Oddershede, J. (1986). Radiative lifetime of the "forbidden" $a^1\Pi_g$← $X^1\Sigma_g$+ transition of N2. *Phys. Scr.* 33, 135–140. doi:10.1088/0031-8949/33/2/007

Deslandres, H. (1902). On the band spectra of nitrogen//C. *R. Acad. Sci.* 134, 747–750.

Frisch, M. J., Trucks, G. W., Schlegel, H. B., Scuseri, G. E., Robb, M. A., Cheeseman, J. R., et al. (2010). *Gaussian, inc., Gaussian 09, revision C.01*. Wallingford CT.

Herzberg, H. (1952). *Spectra of diatomic molecules*. Van Nostrand.

Hochlaf, M., Ndome, H., and Hammoutène, D. (2010). Quintet electronic states of N_2. *J. Chem. Phys.* 132, 104310. doi:10.1063/1.3359000

Hochlaf, M., Ndome, H., Hammoutene, D., and Vervloet, M. (2010). Valence Rydberg electronic states of N_2: Spectroscopy and spin-orbit couplings. *J. Phys. B At. Mol. Opt. Phys.* 43, 245101. doi:10.1088/0953-4075/43/24/245101

Klotz, R., and Peyerimhoff, S. D. (1986). Theoretical study of the intensity of the spin- or dipole forbidden transitions between the c $^1\Sigma^-_u$, A$'$ $^3\Delta_u$, A $^3\Sigma^+_u$ and X $^3\Sigma^-_g$, a$^1\Delta_g$, b$^1\Sigma_g$ states in O_2. *Mol. Phys.* 57, 573–594. doi:10.1080/00268978600100421

Lewis, B. R., Baldwin, G. H., Heays, A. N., Gibson, S. T., Sprengers, J. P., Ubachs, W., et al. (2008). Structure and predissociation of the 3pσ_uD$^3\Sigma_u^+$ Rydberg state of N_2: First extreme-ultraviolet and new near-infrared observations, with coupled-channels analysis. *J. Chem. Phys.* 129, 204303. doi:10.1063/1.3023034

Loboda, O., Minaev, B., Vahtras, O., Schimmelpfennig, B., Ågren, H., Ruud, K., et al. (2003). *Ab initio* calculations of zero-field splitting parameters in linear polyacenes. *Chem. Phys.* 286 (1), 127–137. doi:10.1016/S0301-0104(02)00914-X

Lofthus., A., and Krupenie, P. H. (1977). The spectrum of molecular nitrogen. *J. Phys. Chem. Ref. Data* 6, 113–307. doi:10.1063/1.555546

Minaev, B. F., Knuts, S., Ågren, H., and Vahtras, O. (1993). The vibronically induced phosphorescence in benzene. *Chem. Phys.* 175, 245–254. doi:10.1016/0301-0104(93)85153-Y

Minaev, B. F., Lunell, S., and Kobzev, G. I. (1994). Collision-Induced intensity of the b$^1\Sigma_g^+$–a$^1\Delta_g$ transition in molecular oxygen: Model calculations for the collision complex $O_2 + H_2$. *Int. J. Quantum Chem.* 50 (4), 279–292. doi:10.1002/qua.560500405

Minaev, B. F., and Minaeva, V. A. (2001). MCSCF response calculations of the excited states properties of the O2 molecule and a part of its spectrum. *Phys. Chem. Chem. Phys.* 3, 720–729. doi:10.1039/b006712l

Minaev, B. F., and Muldakhmetov, Z. M. (1984). Influence of spin-orbit interaction on the intensity of optical doublet-doublet and triplet-triplet transitions in molecules. *Opt. Spectrosc.* 56 (1), 27–31.

Minaev, B. F., Norman, P., Jonsson, D., and Ågren, H. (1995). Response theory calculations of singlet-triplet transitions in molecular nitrogen. *Chem. Phys.* 190, 11–29. doi:10.1016/0301-0104(94)00321-Z

Minaev, B. F., Panchenko, A. A., and Hochlaf, M. (2022). Prediction of new emission band $1^3\sum_g^- \rightarrow A^3\sum_u^+$ in the spectrum of nitrogen molecule. *Sci. Tech. Today* 4, 321–338. doi:10.52058/2786-6025-2022-4(4

Minaev, B. F., and Panchenko, A. A. (2020). New aspects of the airglow problem and reactivity of the dioxygen quintet $O_2(^5P_g)$ state in the MLT region as predicted by DFT calculations. *J. Phys. Chem. A* 124, 9638–9655. doi:10.1021/acs.jpca.0c07310

Ndome, H., Hochlaf, M., Lewis, B. R., Heays, A. N., Gibson, S. T., and Lefebvre-Brion, H. (2008). Sign reversal of the spin-orbit constant for the C $^3\Pi_u$ state of N_2. *J. Chem. Phys.* 129, 164307. doi:10.1063/1.2990658

Ni, C., Cheng, J., and Cheng, X. (2017). *Ab initio* calculations for the first-positive bands of N2. *J. Mol. Spectrosc.* 331, 17–22. doi:10.1016/j.jms.2016.10.013

Partridge, H., Langhoff, S. R., Bauschlicher, C. W., and Schwenke, D. W. (1988). Theoretical study of the A$^{'5}\Sigma_g^+$ and C$'^5\Pi_u$ states of N_2: Implications for the N_2 afterglow. *J. Chem. Phys.* 88, 3174–3186. doi:10.1063/1.453962

Piper, L. G. (1993). Reevaluation of the transition-moment function and Einstein coefficients for the N_2 (A$^3\Sigma_u^+$–X$^1\Sigma_g^+$) transition. *J. Chem. Phys.* 99, 3174–3181. doi:10.1063/1.465178

Qin, Z., Zhao, J., and Liu, L. (2019). Radiative transition probabilities between low-lying electronic states of N_2. *Mol. Phys.* 117, 2418–2433. doi:10.1080/00268976.2018.1562579

Werner, H.-J., Kalcher, J., and Reinsch, E.-A. (1984). Accurate *ab initio* calculations of radiative transition probabilities between the$^3\Sigma_u^+$, B$^3\Pi_g$, W $^3\Delta$U, B$'^3\Sigma_u^-$ and C $^3\Pi_u$ states of N_2. *J. Chem. Phys.* 81, 2420–2431. doi:10.1063/1.447917

Wilkinson, P. G., and Mulliken, R. S. (1959). Forbidden band systems in nitrogen. II. The a$''^1\Sigma_u^- \leftarrow$X$^1\Sigma_g^+$ system in absorption. *J. Chem. Phys.* 31, 674–679. doi:10.1063/1.1730445

Wilkinson, P. G. (1962). Some unsolved problems in the vacuum ultraviolet. *J. Quant. Spectrosc. Radiat. Transf.* 2, 343–348. doi:10.1016/0022-4073(62)90020-1

Yonker, J. D., and Bailey, S. M. (2019). N_2(A) in the terrestrial thermosphere. *JGR. Space Phys.* 125, e2019JA026508. doi:10.1029/2019JA026508